

Synthesis and Properties of Novel Borondipyrromethene (BODIPY)-Tethered Triphenylamine Conjugates

Yucai Wang,^{A,B} Junxu Liao,^{B,C} Bangying Wang,^{A,B} Hongbiao Chen,^{A,C}
Hongbin Zhao,^B Min Peng,^B and Sujuan Fan^B

^ACollege of Chemistry, Xiangtan University, Hunan 411105, China.

^BCollege of Chemistry and Environmental Engineering, Dongguan University of Technology, Guangdong 523808, China.

^CCorresponding authors. Email: liaojunxu503@sina.com; zhaohbhanlf@163.com

A series of novel donor–acceptor type borondipyrromethene (BODIPY)-tethered triphenylamine conjugates (BDP4–8) containing one or two BODIPY cores attached to a triphenylamine scaffold at the 4- or 4,4'- positions were successfully synthesised via a mild and effective protocol. Their photophysical and electrochemical properties were investigated. The absorption spectra indicated that the meso-substituted BODIPY with triphenylamine did not give rise to an intense intramolecular charge transfer (ICT) and did not effectively extend the conjugated length compared with substitution at the 2,6- and 3,5-positions as previously reported. It is worth noticing that the asymmetric mono-BODIPY-tethered triphenylamine conjugates (BDP5, BDP7) showed an electronic distribution imbalance due to the special 3D propeller shape of triphenylamine resulting in twisted molecular space configurations. In contrast, the symmetric bis-BODIPY-tethered triphenylamine conjugates (BDP4, BDP6, and BDP8) exhibited a balanced electronic distribution. The photoluminescence spectra of these conjugates exhibited significant Stokes shifts (5300–6700 cm⁻¹), which caused fluorescence emission spectra in near-infrared regions. Cyclic voltammograms reveal that the asymmetric mono-BODIPY-tethered triphenylamine conjugates (BDP5, BDP7) have higher LUMO energy levels and lower HOMO energy levels, thus resulting in larger bandgaps than the bis-BODIPY-tethered triphenylamine ones.

Manuscript received: 28 January 2015.

Manuscript accepted: 12 March 2015.

Published online: 22 April 2015.

Introduction

Derivatives of borondipyrromethene (BODIPY) form an important class of dyes subject to considerable interest owing to a unique combination of facile synthesis, stability, high absorption coefficient, and high photoluminescence efficiency.^[1,2] In addition, the spectroscopic and photophysical properties of BODIPY derivatives can be fine-tuned by the attachment of ancillary residues at the appropriate positions of the BODIPY core^[3–6] by carrying out various synthetic reactions on BODIPY derivatives. Recently, they have been shown as promising for a variety of applications including biological labelling,^[7–9] as electroluminescent devices, as tunable laser dyes,^[10] as potential candidates for solid-state solar concentrators,^[11–15] as fluorescent switches^[16–19] and fluorophores in sensors, and as potential photosensitisers in photodynamic therapy of cancer.^[20–23] We have also focussed on triphenylamine (TPA) and its derivatives, which are well known for their 3D propeller shapes, high hole-transporting and good electron-donating capabilities, and have been widely used for hole injecting/transporting materials for organic light-emitting diodes (LEDs) and organic solar cells.^[24,25] Consequently, the combination of BODIPY dyes with a TPA moiety to construct donor–acceptor (D-A) type TPA-BODIPY conjugates for photoelectronic applications has attracted interest. Moreover, we have recently reported BODIPY dyes modified with TPA at the 2,6-positions, which exhibit good absorption and promising photovoltaic properties in organic

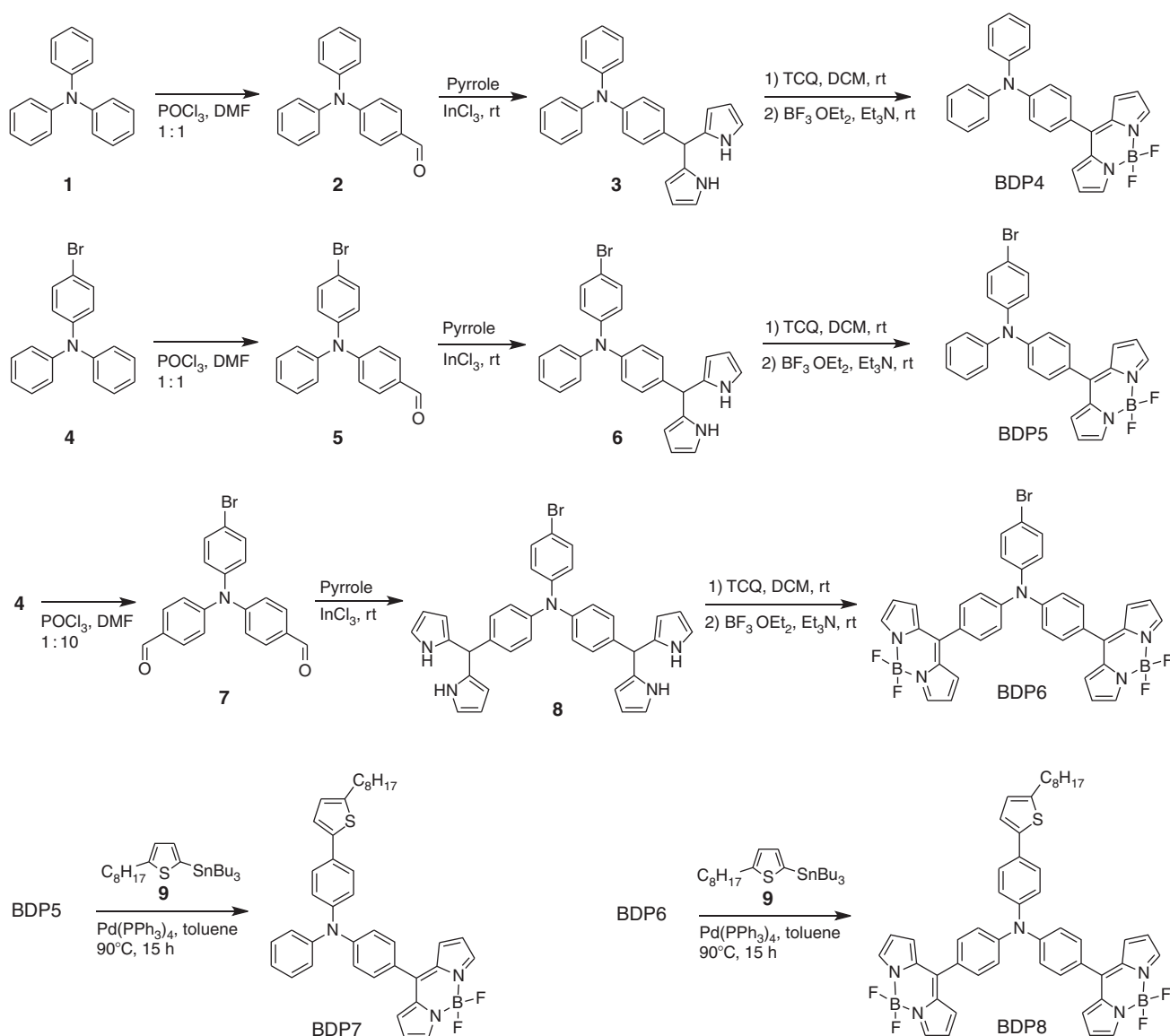
small molecule solar cells.^[26] The 2,6-position TPA-modified dyes benefit from a strong intramolecular charge transfer (ICT), with the absorption spectra exhibiting an obvious red-shift to near-red regions. However, to our best knowledge, TPA-BODIPY conjugates with structural diversity and their resulting property differences have not been systematic studied.

In this paper, we designed and synthesised five novel D-A type BODIPY-tethered TPA conjugates (Scheme 1, BDP4–8) involving one and two BODIPY groups linked at the meso-position to a TPA framework at the 4- and 4,4'-positions, respectively. This novel system was designed in consideration of the following: (i) first, previous studies have shown that functional attachment of BODIPY derivatives with TPA at the 3,5- and 2,6-positions readily result in an obvious ICT. Whether the meso-modified ones possess similar features aroused our interest. (ii) Second, TPA features a 3D propeller shape, whether this structure affects the BODIPY-tethered TPA conjugates and their photophysical and/or electrochemical properties upon introducing different numbers of BODIPY units onto the TPA scaffolding drew our attention.

Results and Discussion

Synthesis and Characterisation

BODIPY-tethered TPA conjugates (BDP4–8) were synthesised according to the route illustrated in Scheme 1. First, according to



Scheme 1. Synthesis of BDP4–8 (rt: room temperature, TCQ: 2,3,5,6-tetrachloro-1,4-benzoquinone).

the previous literature,^[27] mono-formylation of **1** and **4** with POCl_3 and DMF readily afforded aldehydes **2** and **5**. Similarly, dialdehyde **7** was prepared by a bis-formylation reaction from **4**. Subsequently, dipyrromethanes **3**, **6**, and **8** were synthesised from the corresponding aldehydes **2**, **5**, and **7** in a mild way which was reported by our group in 2010.^[28] Finally, a chelating reaction between the dipyrromethanes and $\text{BF}_3\text{-OEt}_2$ in the presence of 2,3,5,6-tetrachloro-1,4-benzoquinone (TCQ) led to the target BODIPY derivatives BDP4–6. The desired BDP7 and BDP8 were obtained by Stille coupling reactions between tributyl(5-octylthiophen-2-yl)stannane (**9**) and BDP5 and BDP6, respectively. All these intermediates and the novel final BODIPY-tethered TPA conjugates are readily available.

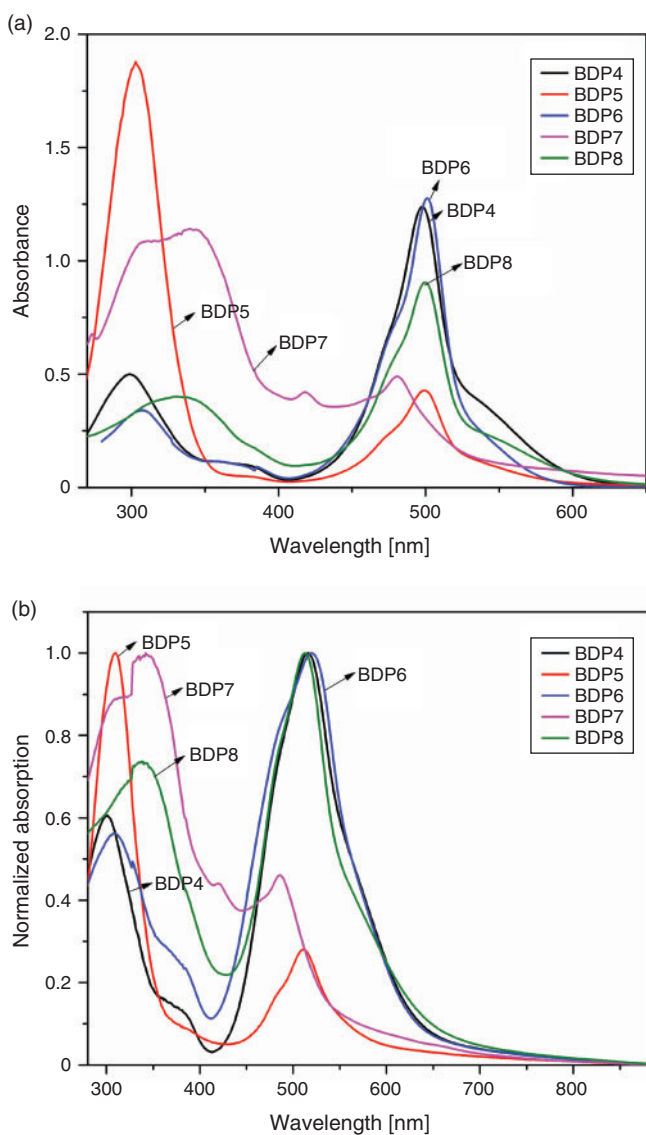
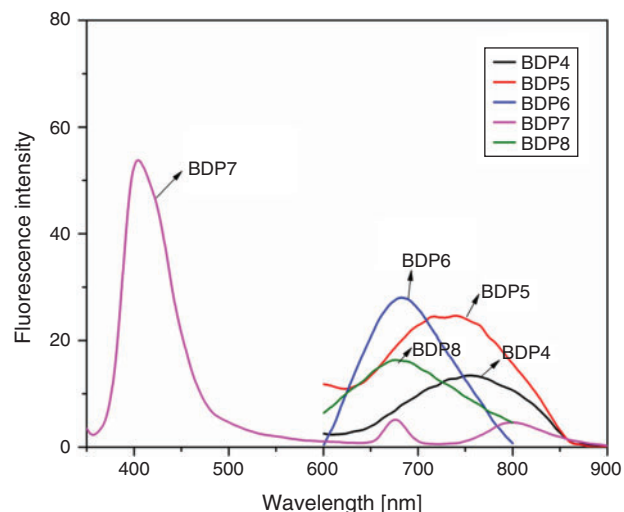
UV-Visible Absorption Spectroscopy

With these novel BODIPY derivatives in hand, we first used UV-vis and fluorescence spectroscopy to investigate their photophysical properties in dilute CH_2Cl_2 solution and in thin films on quartz plates. The UV-vis and photoluminescence properties of these BODIPY derivatives are summarised in

Table 1. Fig. 1 shows the UV-vis absorption spectra of the BODIPY-tethered TPA conjugates (BDP4–8) in diluted CH_2Cl_2 solution ($10^{-5} \text{ mol L}^{-1}$) and as a thin film. All these conjugates show two distinct absorption bands. The first absorption regions from 250 to 350 nm and centred at 300 nm in BDP4–6 can be identified as the $n\text{-}\pi^*$ electronic absorption bands of the TPA moiety, while the first absorption regions from 250 to 400 nm and centred at ~ 350 nm in BDP7–8 were ascribed to the $\pi\text{-}\pi^*$ transition bands derived from the TPA and thiophene fragments. The second absorption bands of these conjugates in the long wavelength regions with $\lambda_{\text{abs,max}}$ at 498, 500, 502, 483 and 501 nm, respectively, can be attributed to the faint ICT interaction between the donor (TPA units) and the acceptor (BODIPY units). Compared with the TPA-BODIPY dyads of structurally substituted BODIPY with TPA at the 2,6- and 3,5-positions, which exhibited an apparent red-shift at ~ 500 nm in absorption spectra, the conjugates featured here with BODIPY units *meso*-tethered to the TPA moiety show a similar absorption profile to that of a free BODIPY dye in solution. These results can be explained in that the intense electronic couplings between

Table 1. Photophysical properties of BDP4–8 at room temperature

Entry	Solution ^A			Film ^B	
	$\lambda_{\text{abs,max}}^{\text{C}}$ [nm]	$\log \epsilon^{\text{D}}$	$\lambda_{\text{em,max}}^{\text{E}}$ [nm]	$\lambda_{\text{abs,max}}^{\text{C}}$ [nm]	$\lambda_{\text{onset}}^{\text{F}}$ [nm]
BDP4	498	5.12	758	516	676
BDP5	500	4.60	738	512	615
BDP6	502	5.21	684	523	678
BDP7	483	4.69	675, 800	489	577
BDP8	501	5.04	682	514	667

^AIn CH₂Cl₂.^BDeposited onto quartz substrate from CH₂Cl₂ solution by the spin-coating technique.^C $\lambda_{\text{abs,max}}$: maximum absorption wavelength of BDPs in CH₂Cl₂ solution or film.^D $\log \epsilon$: logarithmic molar absorption coefficient of BDPs in CH₂Cl₂ solution.^E $\lambda_{\text{em,max}}$: maximum emission wavelength of BDPs in CH₂Cl₂ solution.^F λ_{onset} : absorption threshold from absorption spectra of BDPs in thin film.**Fig. 1.** Normalised UV-vis absorption spectra of BDP4–8 in (a) dilute CH₂Cl₂ solution and (b) thin film.**Fig. 2.** Normalised fluorescence spectra of BDP4–8 in dilute CH₂Cl₂ solution.

the TPA and BODIPY units did not occur. In other words, the effective conjugated length was not obviously increased by attachment of BODIPY to the TPA scaffolding.

On the other hand, it is worth noticing that structurally asymmetric BDP5 and BDP7 show the first absorption bands at 300 and 350 nm, respectively, as main absorption bands, while the other structurally symmetric derivatives BDP4, BDP6, and BDP8 exhibited the second absorption bands as the main band. This phenomenon is probably related to the asymmetric molecular structures breaking the ICT of the donor and acceptor. Since TPA has a 3D propeller shape configuration, substitution at one phenyl ring of the TPA moiety with BODIPY distorted the normal ICT in the total molecule, which decreased the electronic transition probability, thus caused a hypochromic effect. For example, in comparison to BDP4, the introduction of Br onto another phenyl ring of the TPA moiety to give BDP5 led to a hypochromic effect, and the characteristic absorption of BODIPY at ~500 nm was obviously weakened. Interestingly, two BODIPY moieties tethered to TPA (BDP6) enables the whole intermolecular electronic transition to recover to a balanced state (Fig. 1). Similarly, the BODIPY-tethered TPA conjugates BDP7 and BDP8, which feature installation of an electron-rich thiophene unit in another phenyl ring of the TPA framework, also exhibited the same results.

In comparison with the absorption spectra of the BODIPY derivatives in CH₂Cl₂ solutions, these dyes in solid film displayed broadened and red-shifted absorption peaks at 516, 512, 523, 489, and 514 nm, respectively (Fig. 1, Table 1). The results indicated that the effective conjugated length increased for the BODIPY derivatives through 3D π - π stacking.

Fluorescence Spectroscopy of the BODIPY Derivatives

The fluorescence properties of all these BODIPY-tethered TPA conjugates (BDP4–8) were studied in CH₂Cl₂ solution ($c = 10^{-7}$ mol L⁻¹) at room temperature. The normalised fluorescence spectra of them are shown in Fig. 2. To our surprise, except for BDP7, the other BODIPY-tethered TPA conjugates show a significant Stokes shifts (5300–6700 cm⁻¹) resulting in maximum emission peaks at 758, 738, 684, and 682 nm, respectively (Table 1 and Fig. 2). This can be explained on the basis of a photoinduced energy transfer from the BODIPY π - π^*

excited state to the lower lying singlet excited state of TPA and/or to the existence of new non-radiative pathways from the BODIPY $\pi-\pi^*$ state to the ground state, and this process increased phonon coupling.^[29] The results show the promise for practical applications of these BODIPY-tethered TPA

conjugates as near-infrared fluorescence emission materials. BDP7 was also excited at the maximum absorption peak ($\lambda_{\text{abs,max}} = 483 \text{ nm}$), although there were two small emission peaks at 675 and 800 nm, respectively, while an anti-Stokes shift phenomenon was observed to result in a maximum emission peak at 404 nm (Fig. 2). This may be caused by the unbalance of donor and acceptor moieties and the twisted molecular configuration, which inhibited the intramolecular electron transfer. On the other hand, BDP4–8 gave low fluorescent quantum yields. This could be attributed to the increased internal conversion according to the energy gap law that states that the non-radiative deactivation probability of S_0-S_1 increases as the energy gap of S_0-S_1 decreases in a highly extended conjugating system.

Electrochemical Properties of the BODIPY Derivatives

In order to investigate the electrochemical behaviours of these BODIPY-tethered TPA conjugates, the electronic states of compounds BDP4–8 were studied by cyclic voltammetry in CH_2Cl_2 (Fig. 3) and the results are summarised in Table 2. The potentials are reported versus ferrocene as an internal standard and potentials were calibrated by addition of 0.63 eV to the potential (versus scanning calomel electrode, SCE) versus Fc/Fc^+ . It can be seen that the $E_{\text{onset}}^{\text{ox}}$ and E_{p}^{ox} of the five conjugated dyes were all measured at around 1.16 and 1.27 eV, respectively, except for BDP4 (Table 2), indicating that the different groups substituted on the TPA moiety had an obvious effect on the E^{ox} . Their corresponding HOMO (highest occupied molecular orbital) energy level was calculated as approximately -5.6 eV from the equation $E_{\text{HOMO}} = E_{\text{onset}}^{\text{ox}} + 4.4 \text{ eV}$. The results suggest that these BODIPY-tethered TPA conjugates are actually located at a higher energy than we previously reported for BODIPY derivatives substituted with TPA moieties at the 2,6-positions (around -5.35 eV), implying that the HOMO level is sensitive to the positions of the TPA substituent on the BODIPY core of these dyes, which is consistent with the spectroscopic analysis results above. By neglecting any entropy change during light absorption, the reduction potential versus the normal hydrogen electrode (NHE) (E_{red}), which corresponds to the lowest unoccupied molecular orbital (LUMO versus NHE), can be obtained from $E_{\text{onset}}^{\text{ox}}$ and E_{g} , and the calculation results are listed.

Conclusion

In summary, a series of novel BODIPY-tethered TPA conjugates (BDP4–8) containing one or two BODIPY cores attached onto a TPA scaffold at the 4- and 4,4'- positions were

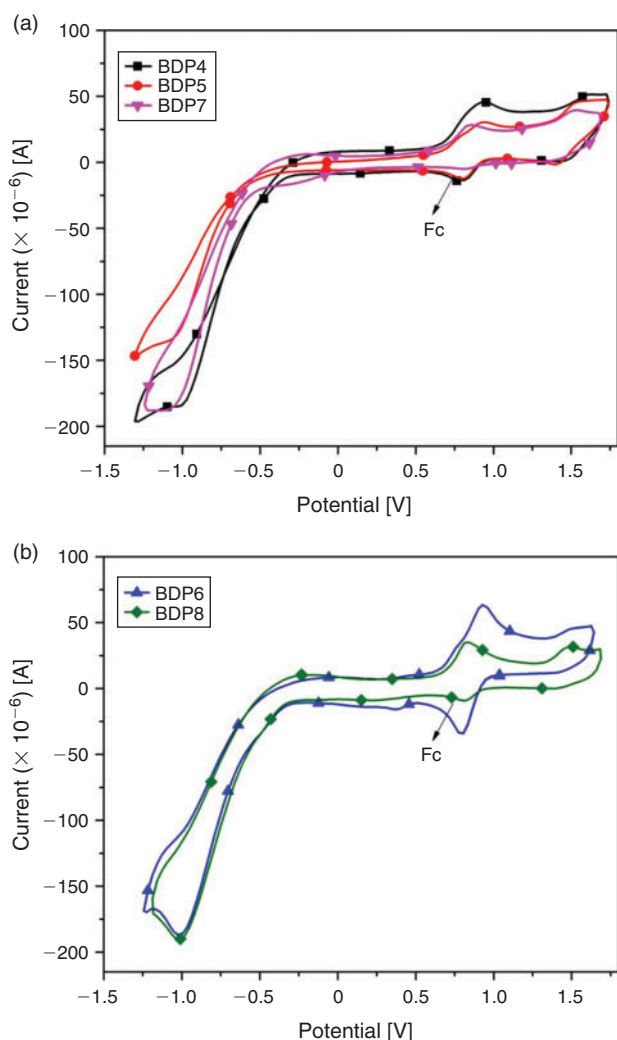


Fig. 3. Cyclic voltammograms of (a) BDP4, BDP5, and BDP7 and (b) BDP6 and BDP8 in CH_2Cl_2 , containing 0.1 M $n\text{-Bu}_4\text{NPF}_6$ as the supporting electrolyte recorded at a scan speed of 50 mV s^{-1} . Fc^+/Fc refers to the ferricinium/ferrocene couple used as internal reference.

Table 2. Solution electrochemical properties of BDP4–8

Entry	E_{g}^{A} [eV]	$E_{\text{onset}}^{\text{oxB}}$ [eV]	$E_{\text{p}}^{\text{oxC}}$ [V]	$E_{\text{red}}^{\text{D}}$ [V] vs NHE	HOMO/LUMO ^E [eV]
BDP4	1.83	1.25	1.35	-1.28	-5.65/-3.82
BDP5	2.01	1.17	1.27	-1.32	-5.57/-3.56
BDP6	1.83	1.14	1.26	-1.27	-5.54/-3.81
BDP7	2.15	1.19	1.31	-1.30	-5.59/-3.44
BDP8	1.86	1.15	1.27	-1.23	-5.55/-3.69

^AEnergy bandgap, determined from UV-vis absorption spectra. At absorption maxima ($E_{\text{g}} = 1240/\lambda_{\text{onset}}$).

^B $E_{\text{onset}}^{\text{ox}}$, onset oxidation potential.

^C E_{p}^{ox} , oxidation peak potential.

^D $E_{\text{red}}^{\text{D}}$, the reduction potential.

^EHOMO = $-(E_{\text{onset}}^{\text{ox}} + 4.4 \text{ eV})$; LUMO = HOMO + E_{g} eV.

successfully synthesised. The absorption spectra indicated that the *meso*-substituted BODIPY with TPA did not give rise to an intense ICT and did not extend the effective conjugated length obviously. It was worth noticing that the asymmetric mono-BODIPY-tethered TPA conjugates (BDP5, BDP7) showed an electronic distribution imbalance due to the special 3D propeller shape of the TPA which resulted in a twisted molecular configuration. In contrast, the symmetric bis-BODIPY-tethered TPA conjugates (BDP4, BDP6, and BDP8) showed a balanced electronic distribution. The photoluminescence spectra of these conjugates exhibited significant Stokes shifts ($5300\text{--}6700\text{ cm}^{-1}$) and caused fluorescence emission spectra in near-infrared regions, as such they show promise for practical applications in near-infrared fluorescence emission materials. Cyclic voltammograms reveal that the asymmetric mono-BODIPY-tethered TPA conjugates (BDP5, BDP7) have higher LUMO energy levels and lower HOMO energy levels than the bis-BODIPY-tethered TPA ones.

Experimental

Materials

TPA, 4-bromo-*N,N*-diphenylaniline, tributyl(5-octylthiophen-2-yl)stannan pyrrole, and phosphorus oxychloride were purchased from Alfa Aesar. Dichloromethane, toluene, and *N,N*-dimethylformamide (DMF) were dried by the accustomed methods and distilled before use. Pyrrole was distilled over CaH_2 before use. All other chemical materials were of reagent grade and used as received without further purification. All chromatographic separations were carried out on silica gel (300–400 mesh).

Instrumentation

^1H and ^{13}C NMR spectra were recorded on a Bruker Avance spectrometer (400 and 101 MHz, respectively) with tetramethylsilane (TMS) as the internal standard. Matrix-assisted laser desorption–ionisation time of flight mass spectra (MALDI-TOF-MS) were recorded on a Bruker Ultraflex-II spectrometer, using an α -cyano-4-hydroxy-cinnamic acid (α -CHCA) matrix. Absorption spectra were recorded on an SHIMADZU UV-2550 UV-Vis spectrophotometer and emission spectra were recorded by using a Hitachi F-4500 instrument. Excitation and emission spectra were fully corrected by reference to a standard lamp. Electrochemical studies made use of cyclic voltammetry (CV) with a conventional three electrode system using a BAS 100W electrochemical analyser in deoxygenated and anhydrous CH_2Cl_2 at room temperature. The potentials are reported versus ferrocene as an internal standard and potentials are calculated relative to SCE assuming $E_{1/2} \text{Fc/Fc}^+ = 0.63\text{ V}$ versus SCE using a scan rate of 100 mV s^{-1} , a glassy carbon working electrode, a $\text{Hg}_2\text{Cl}_2/\text{KCl}$ reference electrode, a platinum counter electrode, and the sample solutions contained $1.0 \times 10^{-3}\text{ M}$ sample and 0.1 M tetrabutylammonium hexafluorophosphate as a supporting electrolyte.

Synthesis

4-(Diphenylamino)benzaldehyde (2)

According to the literature,^[27] to a solution of TPA (980 mg, 4 mmol) and DMF (2 mL) was added POCl_3 (1.8 mL, 4 mmol) dropwise at 0°C with stirring. During this process, a precipitate was formed. After addition was completed, the mixture was warmed to 45°C , and was stirred at this temperature for 2 h. The

mixture was cooled to room temperature and poured into water (10 mL). A yellow precipitate was then formed by adjustment of the pH of the solution to 7 with saturated Na_2CO_3 . This suspension was filtered to give a yellow solid. Recrystallisation from ethanol afforded a needle-like pale yellow solid (1.00 g, yield 92%). δ_{H} (400 MHz, CDCl_3 , TMS) 9.86 (s, 1H), 7.71–7.73 (d, J 8.0, 2H), 7.11–7.40 (m, 10H), 7.04–7.06 (d, J 8.2, 2H). The characterisation data were consistent with the literature.

4-((4-Bromophenyl)(phenyl)amino)benzaldehyde (5)

The aldehyde **5** was synthesised by a similar procedure to prepare aldehyde **2** using **4** as a reactant. The desired compound **5** was obtained as a pale yellow solid in 89% yield. δ_{H} (400 MHz, CDCl_3 , TMS) 9.85 (s, 1H), 7.71 (d, J 8.0, 2H), 7.47 (d, J 8.0, 2H), 7.39–7.35 (m, 2H), 7.23–7.16 (m, 3H), 7.07–7.03 (m, 4H). δ_{C} (101 MHz, CDCl_3) 190.4, 152.9, 145.9, 145.4, 132.8, 131.4, 130.2, 129.9, 127.4, 126.3, 125.4, 120.0, 117.7. The characterisation data were consistent with the literature.^[30]

4,4'-((4-Bromophenyl)azanediyl)dibenzaldehyde (7)

According to the literature,^[31] to a solution of 4-bromo-*N,N*-diphenylaniline (650 mg, 2 mmol) and DMF (5 mL) was added POCl_3 (9 mL, 20 mmol) dropwise at 0°C with stirring, during this process, a precipitate was formed. After addition was completed, the mixture was warmed to 45°C and stirred at this temperature for 2 h. The mixture was cooled to room temperature, poured into water (20 mL), and extracted with CH_2Cl_2 (20 mL \times 2). The organic extracts were washed with brine (20 mL \times 2) and water (20 mL \times 2), dried with anhydrous Na_2SO_4 , and concentrated. The residue was purified by silica gel column chromatography (petroleum ether/ CH_2Cl_2 , 10 : 1) to give the desired **7** as a light yellow solid (618 mg, yield 81%). δ_{H} (400 MHz, CDCl_3 , TMS) 9.88 (s, 2H), 7.80–7.78 (d, J 8.0, 4H), 7.15–7.50 (m, 6H), 7.04–7.06 (d, J 8.2, 2H). The characterisation data were consistent with the literature.^[31]

4-(Di(1H-pyrrol-2-yl)methyl)-*N,N*-diphenylaniline (3)

According to the literature,^[28] a mixture of pyrrole (14 mL, 150 mmol) and 4-(diphenylamino)benzaldehyde (**2**) (546 mg, 2.0 mmol) was treated with InCl_3 (44 mg, 0.2 mmol) at room temperature under argon. After stirring for 2 h, powdered NaOH (400 mg, 10 mmol) was added to terminate the reaction. The literature procedure was then followed to give a brown solid (750 mg). This solid was used directly for the next step without further purification.

4-Bromo-*N*-(4-(di(1H-pyrrol-2-yl)methyl)phenyl)-*N*-phenylaniline (6)

Dipyrrromethane **6** was synthesised by a similar procedure for preparing dipyrrromethane **3**. A mixture of pyrrole (14 mL, 150 mmol) and dialdehyde **5** (704 mg, 2 mmol) was treated with InCl_3 (44 mg, 0.2 mmol) at room temperature under argon. After stirring for 2 h, powdered NaOH (400 mg, 10 mmol) was added to terminate the reaction. Pyrrole was removed under reduced pressure, and the residue was purified by silica gel column chromatography (petroleum ether/ CH_2Cl_2 , 1 : 1) to give the desired product **3** as a pale brown solid (935 mg, yield 91%). δ_{H} (400 MHz, DMSO) 7.95 (s, 2H), 7.31 (d, J 7.7, 2H), 7.24 (d, J 7.4, 2H), 7.09–7.07 (m, 3H), 7.04 (d, J 8.8, 2H), 6.99 (d, J 8.0, 2H), 6.93 (d, J 7.8, 2H), 6.70 (s, 2H), 6.16 (s, 2H), 5.93 (s, 2H),

5.41 (s, 1H). δ_C (101 MHz, DMSO) 147.29, 146.93, 146.13, 136.80, 132.64, 132.22, 129.47, 129.32, 125.23, 124.54, 124.20, 123.40, 117.37, 114.90, 108.46, 107.24, 43.42. m/z (MALDI-TOF-MS) 467.135. Calc. for $C_{27}H_{22}BrN_3$: 467.100.

4-Bromo-N,N-bis(4-(di(1H-pyrrol-2-yl)methyl)phenyl)aniline (8)

The dipyrromethane **8** was synthesised by a similar procedure for preparing dipyrromethane **3** using dialdehyde **7** as reactant. The desired product **8** was obtained as a pale brown solid (yield 88%). δ_H (400 MHz, DMSO) 7.95 (s, 4H), 7.31 (d, J 8.1, 2H), 7.09 (d, J 7.5, 4H), 6.99 (d, J 7.5, 4H), 6.93 (d, J 7.9, 2H), 6.71 (s, 4H), 6.16 (s, 4H), 5.92 (s, 4H), 5.42 (s, 2H). δ_C (101 MHz, $CDCl_3$) 146.80, 146.02, 136.98, 132.59, 132.22, 129.34, 125.11, 124.37, 117.36, 114.90, 108.46, 107.24, 43.41.

BDP4

The dipyrromethane **3** (750 mg, crude) was dissolved in CH_2Cl_2 (50 mL), and to the solution was added TCQ (492 mg, 2 mmol) at room temperature. After stirring for 8 h, $BF_3 \cdot Et_2O$ (4 mL, 30 mmol) and Et_3N (4 mL, 28 mmol) were added in that order under a nitrogen flow and the reaction was allowed to proceed at room temperature for 3 h. The reaction mixture was then diluted with ethyl ether and repeatedly washed with water. The organic layer was dried over anhydrous sodium sulfate, concentrated under vacuum, and the residue was purified by silica gel column chromatography (petroleum ether/ CH_2Cl_2 , 1 : 1) to give the final product as a purple solid with a metallic luster (442 mg, yield 50%). Mp 223–224°C. δ_H (400 MHz, $CDCl_3$ TMS) 7.90 (s, 2H), 7.45–7.47 (d, J 8.4, 2H), 7.06–7.36 (m, 14H), 6.55 (s, 2H). δ_C (100 MHz, $CDCl_3$, TMS) 148.67, 147.73, 144.61, 135.62, 134.76, 133.67, 132.30, 130.36, 129.80, 128.47, 127.44, 127.28, 126.90, 122.76, 119.06, 117.25. m/z (MALDI-TOF-MS) 435.329. Calc. for $C_{27}H_{20}BF_2N_3$: 435.040.

BDP5

The synthesis procedure of BDP5 was similar to BDP4. The desired BDP5 was obtained as a purple solid with a metallic luster with 58% yield. Mp 208–210°C. δ_H (400 MHz, $CDCl_3$) 7.91 (s, 2H), 7.47 (d, J 7.7, 2H), 7.45 (d, J 7.8, 2H), 7.36 (d, J 7.6, 2H), 7.21–7.19 (m, 3H), 7.11 (d, J 8.8, 2H), 7.09 (d, J 9.0, 2H), 7.05 (s, 2H), 6.56 (s, 2H). δ_C (101 MHz, $CDCl_3$) 150.42, 146.16, 145.72, 143.08, 134.65, 133.42, 132.76, 132.34, 131.15, 129.90, 127.05, 126.85, 126.00, 125.09, 120.60, 118.16, 117.22. m/z (MALDI-TOF-MS) 494.159 ($[M - F]^+$). Calc. for $C_{27}H_{19}BBBrF_2N_3$: 513.081. HRMS m/z 494.0854 ($[M - F]^+$); calc. for $C_{27}H_{19}BBBrF_2N_3$ 494.0839 ($[M - F]^+$).

BDP6

To a solution of **8** (306 mg, 0.5 mmol) in CH_2Cl_2 (50 mL) was added TCQ (246 mg, 1 mmol) at room temperature. After stirring for 8 h, $BF_3 \cdot Et_2O$ (3 mL, 22 mmol) and Et_3N (3 mL, 21 mmol) were added in that order under a nitrogen flow and the reaction was allowed to proceed at room temperature for 3 h. The reaction mixture was then diluted with ethyl ether and repeatedly washed with water. The organic layer was dried over anhydrous sodium sulfate. The crude product was then concentrated under vacuum and purified by silica gel column chromatography (petroleum ether/ CH_2Cl_2 , 2 : 1). The red coloured fraction was collected and the solvent was removed under reduced pressure to give the final product as a purple solid with a metallic luster (265 mg, yield 75%). Mp 276–278°C.

δ_H (400 MHz, $CDCl_3$) 7.95 (s, 4H), 7.57–7.55 (m, 6H), 7.28 (d, J 9.9, 4H), 7.18 (d, J 8.1, 2H), 7.05 (s, 4H), 6.58 (s, 4H). δ_C (100 MHz, $CDCl_3$, TMS) 149.24, 146.66, 145.11, 143.72, 134.75, 133.30, 132.36, 131.16, 128.84, 128.07, 122.82, 118.79, 118.40. m/z (MALDI-TOF-MS) 684.148 ($[M - F]^+$). Calc. for $C_{36}H_{24}B_2BrF_4N_5$: 703.13. HRMS m/z 684.1369 ($[M - F]^+$); calc. for $C_{36}H_{24}B_2BrF_4N_5$ 684.1353 ($[M - F]^+$).

BDP7

To a solution of BDP5 (200 mg, 0.39 mmol) and tributyl(5-octylthiophen-2-yl)stannane (**9**) (200 mg, 0.41 mmol) in toluene (20 mL) was added $Pd(PPh_3)_4$ (116 mg, 0.10 mmol). The mixture was stirred at 90°C for 15 h under an Ar atmosphere. The reaction mixture was then cooled to room temperature, poured into water (40 mL), and extracted with CH_2Cl_2 (20 mL \times 2). The organic layer was dried over anhydrous sodium sulfate and concentrated under vacuum. The resultant residue was purified by silica gel column chromatography (petroleum ether/ethyl acetate, 15 : 1) to give the desired BDP7 as a purple solid (186 mg, yield 76%). Mp 93–95°C. δ_H (400 MHz, $CDCl_3$) 7.90 (s, 2H), 7.52 (d, J 8.5, 2H), 7.47 (d, J 8.7, 2H), 7.36 (t, J 7.8, 2H), 7.23 (d, J 7.6, 2H), 7.20–7.16 (m, 3H), 7.14 (d, J 8.7, 2H), 7.09 (d, J 3.5, 1H), 7.06 (d, J 3.8, 2H), 6.74 (d, J 3.4, 1H), 6.55 (d, J 2.3, 2H), 2.82 (t, J 7.5, 2H), 1.76–1.63 (m, 2H), 1.43–1.21 (m, 10H), 0.88 (t, J 5.9, 3H). δ_C (101 MHz, $CDCl_3$) 150.73, 146.33, 145.77, 145.26, 142.87, 140.92, 134.65, 132.38, 131.22, 131.09, 129.80, 129.75, 126.66, 126.50, 126.01, 125.93, 125.14, 124.89, 122.55, 120.38, 120.06, 118.07, 33.78, 31.90, 30.31, 29.27, 27.88, 26.88, 22.70, 14.15. m/z (MALDI-TOF-MS) 582.460 ($[M - 47]^+$). Calc. for $C_{39}H_{38}BF_2N_3S$: 629.282. HRMS m/z 610.2880 ($[M - F]^+$); calc. for $C_{39}H_{38}BF_2N_3S$ 610.2864 ($[M - F]^+$).

BDP8

The BDP8 was prepared according to a similar procedure for preparing BDP7 using BDP6 as reactant. The desired product BDP8 was obtained as a purple solid (yield 81%). Mp 120–122°C. δ_H (400 MHz, $CDCl_3$) 7.94 (s, 4H), 7.61 (d, J 8.5, 2H), 7.56 (d, J 8.6, 4H), 7.31 (d, J 8.6, 4H), 7.26 (d, J 6.9, 2H), 7.14 (d, J 3.5, 1H), 7.07 (d, J 4.0, 4H), 6.77 (d, J 3.4, 1H), 6.58 (d, J 4.0, 4H), 2.84 (t, J 7.6, 2H), 1.75–1.69 (m, 2H), 1.45–1.22 (m, 10H), 0.87 (t, J 3.6, 3H). δ_C (101 MHz, $CDCl_3$) 149.45, 146.82, 144.48, 143.52, 140.49, 134.71, 132.47, 132.32, 131.15, 128.49, 127.00, 126.94, 125.54, 125.20, 122.95, 122.67, 118.32, 33.52, 31.84, 30.27, 29.32, 28.74, 27.12, 22.63, 14.06. m/z (MALDI-TOF-MS) 800.536 ($[M - F]^+$). Calc. for $C_{48}H_{43}B_2F_4N_5S$: 819.282. HRMS m/z 800.3406 ($[M - F]^+$); calc. for $C_{48}H_{43}B_2F_4N_5S$ 800.3377 ($[M - F]^+$).

Supplementary Material

1H and ^{13}C NMR spectra and mass spectra for all unknown compounds are available on the Journal's website.

Acknowledgements

This work was supported by the Natural Science Foundation of Guangdong Province (2014A030313630), the National Nature Science Foundation of China (51476036, 21342003), Project for High-level Personnel of University in Guangdong Province ([2013]246), the University Science and Technology Innovation Key Project of Guangdong Province (cxzd1148), and the University and Scientific Research Institution Key Project of Dongguan City (2012108101005).

References

- [1] G. Ulrich, R. Ziessel, A. Harriman, *Angew. Chem. Int. Ed.* **2008**, *47*, 1184. doi:10.1002/ANIE.200702070
- [2] A. Loudet, K. Burgess, *Chem. Rev.* **2007**, *107*, 4891. doi:10.1021/CR078381N
- [3] M. Vincent, E. Beabout, R. Bennett, P. Hewavitharanage, *Tetrahedron Lett.* **2013**, *54*, 2050. doi:10.1016/J.TETLET.2013.01.128
- [4] C. Zhao, X. Wang, J. Cao, P. Feng, J. Zhang, Y. Zhang, Y. Yang, Z. Yang, *Dyes Pigment.* **2013**, *96*, 328. doi:10.1016/J.DYEPIG.2012.08.026
- [5] V. Leen, D. Miscoria, S. Yin, A. Filarowski, J. Molisho Ngongo, M. Van der Auweraer, N. Boens, W. Dehaen, *J. Org. Chem.* **2011**, *76*, 8168. doi:10.1021/JO201082Z
- [6] W. Qin, V. Leen, W. Dehaen, J. Cui, C. Xu, X. Tang, W. Liu, T. Rohand, D. Beljonne, B. V. Averbeke, J. N. Clifford, K. Driesen, K. Binnemans, M. Van der Auweraer, N. Boens, *J. Phys. Chem. C* **2009**, *113*, 11731. doi:10.1021/JP901782Z
- [7] S. Sankaranarayanan, G. Kellner-Weibel, M. de la Llera-Moya, M. C. Phillips, B. F. Asztalos, R. Bittman, G. H. Rothblat, *J. Lipid Res.* **2011**, *52*, 2332. doi:10.1194/JLR.D018051
- [8] Y. Ohsaki, Y. Shinohara, M. Suzuki, T. Fujimoto, *Histochem. Cell Biol.* **2010**, *133*, 477. doi:10.1007/S00418-010-0678-X
- [9] Y. Ikawa, S. Moriyama, H. Furuta, *Anal. Biochem.* **2008**, *378*, 166. doi:10.1016/J.AB.2008.03.054
- [10] I. García-Moreno, D. Zhang, Á Costela, V. Martín, R. Sastre, Y. Xiao, *J. Appl. Phys.* **2010**, *107*, 073105. doi:10.1063/1.3327437
- [11] O. Altan Bozdemir, S. Erbas-Cakmak, O. O. Ekiz, A. Dana, E. U. Akkaya, *Angew. Chem. Int. Ed.* **2011**, *50*, 10907. doi:10.1002/ANIE.201104846
- [12] S. Kolemen, O. A. Bozdemir, Y. Cakmak, G. Barin, S. Erten-Ela, M. Marszalek, J.-H. Yum, S. M. Zakeeruddin, M. K. Nazeeruddin, M. Gratzel, E. U. Akkaya, *Chem. Sci.* **2011**, *2*, 949. doi:10.1039/C0SC00649A
- [13] S. Kolemen, Y. Cakmak, S. Erten-Ela, Y. Altay, J. Brendel, M. Thelakkat, E. U. Akkaya, *Org. Lett.* **2010**, *12*, 3812. doi:10.1021/OL1014762
- [14] D. Kumaresan, R. P. Thummel, T. Bura, G. Ulrich, R. Ziessel, *Chem. – Eur. J.* **2009**, *15*, 6335. doi:10.1002/CHEM.200900518
- [15] S. Hattori, K. Ohkubo, Y. Urano, H. Sunahara, T. Nagano, Y. Wada, N. V. Tkachenko, H. Lemmetyinen, S. Fukuzumi, *J. Phys. Chem. B* **2005**, *109*, 15368. doi:10.1021/JP050952X
- [16] N. Boens, V. Leen, W. Dehaen, *Chem. Soc. Rev.* **2012**, *41*, 1130. doi:10.1039/C1CS15132K
- [17] J. Shao, H. Sun, H. Guo, S. Ji, J. Zhao, W. Wu, X. Yuan, C. Zhang, T. D. James, *Chem. Sci.* **2012**, *3*, 1049. doi:10.1039/C2SC00762B
- [18] Y. Chen, J. Zhao, H. Guo, L. Xie, *J. Org. Chem.* **2012**, *77*, 2192. doi:10.1021/JO202215X
- [19] F. Puntoriero, F. Nastasi, T. Bura, R. Ziessel, S. Campagna, A. Giannetto, *New J. Chem.* **2011**, *35*, 948. doi:10.1039/C0NJ00770F
- [20] A. Kamkaew, S. H. Lim, H. B. Lee, L. V. Kiew, L. Y. Chung, K. Burgess, *Chem. Soc. Rev.* **2013**, *42*, 77. doi:10.1039/C2CS35216H
- [21] S. G. Awuah, Y. You, *RSC Adv.* **2012**, *2*, 11169. doi:10.1039/C2RA21404K
- [22] H. G. Jang, M. Park, J. S. Wishnok, S. R. Tannenbaum, G. N. Wogan, *Anal. Biochem.* **2006**, *359*, 151. doi:10.1016/J.AB.2006.08.030
- [23] R. P. Haugland, *The Handbook: A Guide to Fluorescent Probes and Labeling Technologies*, 10th edn **2005** (Invitrogen: Eugene, OR).
- [24] Y. Shirota, H. Kageyama, *Chem. Rev.* **2007**, *107*, 953. doi:10.1021/CR050143+
- [25] Z. Ning, H. Tian, *Chem. Commun.* **2009**, 5483. doi:10.1039/B908802D
- [26] H. Zhao, B. Wang, J. Liao, H. Wang, G. Tan, *Tetrahedron Lett.* **2013**, *54*, 6019. doi:10.1016/J.TETLET.2013.08.088
- [27] X.-C. Li, Y. Liu, M. S. Liu, A. K.-Y. Jen, *Chem. Mater.* **1999**, *11*, 1568. doi:10.1021/CM990018C
- [28] H. Zhao, J. Liao, J. Ning, Y. Xie, Y. Cao, L. Chen, D. Yang, B. Wang, *Adv. Synth. Catal.* **2010**, *352*, 3083. doi:10.1002/ADSC.201000336
- [29] W. Qin, V. Leen, T. Rohand, W. Dehaen, P. Dedecker, M. Van der Auweraer, K. Robeyns, L. Van Meerelt, D. Beljonne, B. Van Averbeke, J. N. Clifford, K. Driesen, K. Binnemans, N. Boens, *J. Phys. Chem. A* **2009**, *113*, 439. doi:10.1021/JP8077584
- [30] L. Zhang, Y. Liu, Z. Wang, M. Liang, Z. Sun, S. Xue, *Tetrahedron* **2010**, *66*, 3318. doi:10.1016/J.TET.2010.02.095
- [31] H. Zhao, J. Liao, D. Yang, Y. Xie, Y. Xu, H. Wang, B. Wang, *Aust. J. Chem.* **2013**, *66*, 972. doi:10.1071/CH12521